ISSN: 2414-1895 DOI: 10.6919/ICJE.202504_11(4).0021

Effects of ECAP and Different Aging Processes on the Corrosion Resistance of Maraging Stainless Steel

Yinan Chen

Shanghai University of Technology, Shanghai 200093, China

Abstract

This paper focuses on 1RK91 maraging stainless steel to explore the influence of different Equal Channel Angular Pressing (ECAP) passes and aging processes on its corrosion resistance in a 3.5% NaCl solution. Through electrochemical polarization curve testing and impedance spectroscopy analysis, the results indicate that after ECAP treatment, the corrosion resistance of the samples initially improves and subsequently deteriorates. Samples treated with ECAP-1 and ECAP-2 exhibit superior corrosion resistance, whereas those subjected to ECAP-3 demonstrate the poorest performance due to increased dislocation density and reduced volume fraction of retained austenite. Under conventional aging processes, both solution-treated and ECAP-3-treated samples show optimal corrosion resistance in the T_3 condition and the worst in T_4. Additionally, ECAP-3 samples after conventional aging exhibit better corrosion resistance than solution-treated counterparts under the same aging conditions. For step-aging processes, solution-treated samples achieve the best corrosion resistance in T_8 and the worst in T_5. Conversely, ECAP-3-treated samples display the highest corrosion resistance in T5 and the lowest in T_8. With the exception of the T_8 condition, ECAP-3 samples subjected to step-aging generally exhibit enhanced corrosion resistance compared to solution-treated samples undergoing step-aging. This study provides a reference for selecting optimal treatment processes for 1RK91 maraging stainless steel in industrial applications.

Keywords

1RK91 Maraging Stainless Steel; ECAP ; Aging Process; Corrosion Resistance; Electrochemical Test.

1. Introduction

1RK91 maraging stainless steel exhibits superior corrosion resistance compared to other types of stainless steels. Its carbon content is extremely low, and almost no chromium carbides precipitate during heat treatment, enabling the maintenance of a high concentration of corrosion - resistant chromium elements in the matrix.[1-3] Meanwhile, this steel contains alloying elements such as nickel and molybdenum, which can synergistically interact with chromium to stabilize the chromium oxide (Cr_2O_3) film on the sample surface, further enhancing corrosion resistance. The copper element in the steel also contributes to this. Generally, the corrosion resistance of stainless steels is affected by factors such as alloying elements and impurities, and the processing technology in a specific environment can also affect the stability of the passive film. Although maraging stainless steels have good corrosion resistance, pitting corrosion may still occur in a chloride - ion environment[4-7].

The processing process can significantly change the electrochemical properties of materials. The general view is that processing has a negative impact on the corrosion resistance of carbon steels. During processing, the grains deform, dislocations occur and slip, forming acicular and strip - shaped microstructures, which affect the electrochemical behavior of stainless steels in corrosive media.

ISSN: 2414-1895 DOI: 10.6919/ICJE.202504_11(4).0021

Some studies have shown that moderate processing can improve corrosion resistance, while excessive processing will damage it. For example, when the processing degree of nickel - free high - nitrogen stainless steel reaches 20%, the pitting corrosion performance is improved to some extent. However, some studies also point out that processing is detrimental to the corrosion resistance of materials. For instance, Kurc et al. found that for AISI 304 austenitic stainless steel in the ECAP range of 10% - 70%, with the increase in deformation, the corrosion performance in a 3.5% NaCl solution decreases. Currently, there are few studies on the effect of processing on the corrosion resistance of 1RK91 maraging stainless steel. Since this steel undergoes deformation - induced martensitic transformation and introduces residual stress during cold rolling, it is particularly important to study the influence of cold rolling on its corrosion resistance[8-12].

Aging treatment is a key strengthening process for maraging stainless steels, and studying its impact on the corrosion resistance of materials is of great significance. Existing research has shown that the precipitation of strengthening phases and the reverse transformation of austenite during the aging process significantly affect the corrosion resistance of materials. Jiang Yue et al. carried out an aging treatment on 00Cr13Ni7Co5Mo4W at 450 - 580 °C for 8 hours and found that the higher the aging temperature, the greater the number of precipitation phase R, which promotes the reverse transformation of austenite and thus affects the corrosion resistance. Li Yuansong studied the pitting corrosion behavior of 0Cr15Ni5Cu3Nb stainless steel in a chloride - ion medium and found that the specimens subjected to solution treatment, adjustment, and aging had better corrosion resistance than those directly aged after solution treatment. Ma Jinping et al. pointed out that during the aging of 00Cr15 - 16Ni6Mo2 - 3CuAl, pitting corrosion mainly occurs at the precipitation phases and their original austenite grain boundaries. Due to the growth and coarsening of the precipitation phases, the pitting - corrosion resistance of the original austenite grain boundaries decreases significantly. Currently, research on the effect of aging treatment on the corrosion resistance of 1RK91 maraging stainless steel is insufficient and requires further in - depth exploration[13-17].

This chapter mainly uses electrochemical polarization curves and electrochemical impedance techniques to study the electrochemical corrosion behavior of 1RK91 maraging stainless steel in a 3.5% NaCl solution under different ECAP passes and aging processes, providing a reference for appropriate processing technologies in industrial production.

2. Experimental Methods

First, the steel is solution-treated. Then, using the ECAP equipment, ECAP treatment with different passes is carried out on the solution-treated samples to prepare ECAP-1, ECAP-2, and ECAP-3 samples. The aging treatment includes two processes: conventional aging and step aging. Four conditions, T_1 - T_4, are set for the conventional aging, and four conditions, T_5 - T_8, are set for the step aging. The solution-treated and ECAP-3 processed samples are processed according to different aging processes. The electrochemical corrosion performance of the materials is tested using a CHI600E electrochemical workstation. The square specimens with dimensions of 10 mm×10 mm×1.5 mm cut by wire cutting are used as working electrodes. The specimens are successively polished with 400 - 1500 mesh sandpapers, then polished, ultrasonically cleaned with alcohol, and finally immersed in a 3.5% NaCl solution for 24 h, leaving a test surface of 10 mm×10 mm. During the corrosion test, the stable open-circuit potential (OCP) is measured in the 3.5% NaCl solution for 400 s first. For the potentiodynamic polarization curve parameters: the voltage scanning range is - 0.7 to 0.5 V, and the scanning rate is 10 mV/min. For the electrochemical impedance parameters: the working frequency range is 10^5 to 10^{-2} Hz, the amplitude is 5 mV, and the data is fitted and analyzed using Zsimpwin software.

ISSN: 2414-1895 DOI: 10.6919/ICJE.202504_11(4).0021

Table 1. Martensitic stainless steel aging process

serial number	aging temperature/℃	time/min
T_1	480	120
T_2	500	120
T_3	530	120
T_4	560	120

Table 2. Martensitic stainless steel graded aging process

serial number	temperature/℃	time/min	temperature /℃	time/min
T_5	450	30	480	90
T_6	450	30	500	90
T_7	500	30	530	90
T_8	500	30	560	90

3. Results and Analysis

3.1 Effect of ECAP Pass Number on Corrosion Resistance of 1RK91 Stainless Steel

Fig. 1 presents the polarization curves of 1RK91 maraging stainless steel subjected to different passes of ECAP. The outcomes clearly demonstrate that ECAP exerts a significant influence on the polarization characteristics of the steel. All samples processed by ECAP display the features of a passivation region. In order to analyze these electrochemical properties, the Tafel extrapolation method was adopted in this study to calculate the self - corrosion current density (Icorr) and corrosion potential (Ecorr) of the steel. Among them, (Ecorr) is capable of reflecting whether the material has a tendency towards oxidation or passivation within a corrosive environment. The lower its value, the more readily the anodic reaction will occur (Icorr) represents the corrosion rate of the material. Table 3 tabulates the corrosion potential, self - corrosion current density, and pitting potential (Eb) of the samples under various deformation levels. It is noteworthy that the corrosion potential of samples with different deformation levels is higher than that of the solution - annealed samples.

At low ECAP passes, the self-corrosion current density of the samples initially decreases and then increases. For instance, under ECAP-1, the self-corrosion current density is 0.714×10^{-6} A/cm², which might be attributed to the non - uniform distribution of some microstructures resulting from the overly rapid cooling rate during the solution treatment. After one pass of ECAP, the microstructure becomes more homogeneous, and the self - corrosion current density decreases. When the number of ECAP passes exceeds 1, the self-corrosion current density first decreases and then increases. At ECAP-2, the self - corrosion current density attains the lowest value of 0.583×10^{-6} A/cm²; at ECAP-3, it ascends to the maximum value of 1.779×10^{-6} A/cm². This is because, under the deformation condition of ECAP-2, the proliferation of dislocations leads to the formation of fine lath - shaped martensite structures within the retained austenite, refining the grains and reducing the local corrosion rate. However, when the number of ECAP passes increases to 3, the dislocation density surges sharply, the number of structural defects increases, and the residual stress causes the volume fraction of deformed martensite to reach its peak. Under such circumstances, the interface characteristics between austenite and martensite alter, resulting in diverse corrosion - resistance performances. Generally speaking, the more homogeneous the microstructure, the better the corrosion resistance.

Furthermore, the sample under ECAP-2 exhibits the highest pitting potential, indicating that its surface passivation film is more stable and endows it with better corrosion resistance. In contrast, the sample under ECAP-3 has the highest corrosion current density, signifying a strong corrosion tendency and the poorest corrosion resistance. Once the potential reaches the pitting threshold, pitting

ISSN: 2414-1895 DOI: 10.6919/ICJE.202504_11(4).0021

holes emerge on the surface of the sample. As the current density further increases, the pitting expands, ultimately rupturing the surface passivation film and deteriorating the corrosion resistance.

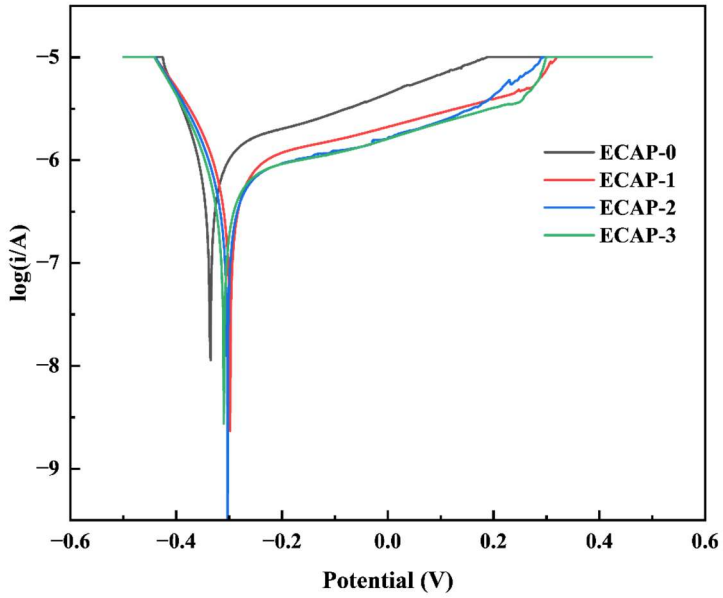

Fig.1 Polarization curves of 1RK91 under different ECAP passes

Fig. 2 shows the Nyquist plots of 1RK91 under different passes of ECAP. According to the frequency range covered by the experimental tests, the impedance plots of all ECAP samples exhibit the characteristic of a single capacitive reactance arc. It is worth noting that the radius of the capacitive reactance arc of the ECAP-2 sample is significantly larger than that of other samples, which usually implies better corrosion resistance. In contrast, the ECAP-3 sample has the smallest radius of the capacitive reactance arc, indicating that its corrosion resistance is the worst among the three.

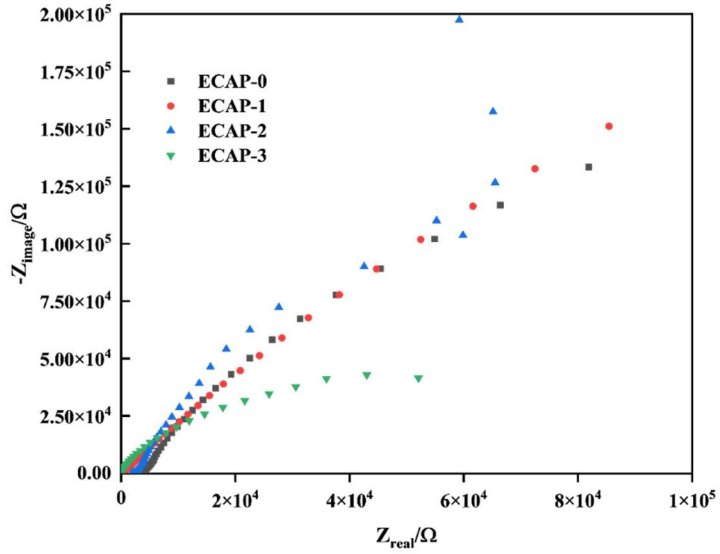

Fig.2 Nyquist plots of 1RK91 under different ECAP passes

ISSN: 2414-1895 DOI: 10.6919/ICJE.202504_11(4).0021

Table 3. Electrochemical params of 1RK91 under different ECAP passes

factor	ECAP-0	ECAP-1	ECAP-2	ECAP-3
$I_{CORR}\times10^{-6}$(A/cm^2)	1.191	0.714	0.583	1.779
E_{CORR}(Vvs.SCE)	-0.317	-0.295	-0.298	-0.307
E_b/V	0.281	0.299	0.348	0.342

3.2 Influence of Conventional Aging Process on the Corrosion Resistance of 1RK91 Stainless Steel

Fig. 3 shows the polarization curves of 1RK91 after conventional aging. Solution-treated samples show a distinct passivation range, indicating a stable passivation film on the surface. Table 4 lists self-corrosion current density Icorr and corrosion potential Ecorr under different aging processes. For T_1 and T_2 aging, Icorr values are 0.323×10^{-6} A/cm² and 0.386×10^{-6} A/cm². The T_2 process increases the corrosion rate and reduces corrosion resistance due to the precipitation of Ni_3Ti and Fe_2Mo, which lower Ni and Mo in the matrix, weakening the passivation film. The Icorr of the T1 - treated sample is lower than that of the solution - treated one 1.191×10^{-6} A/cm², possibly because T1 - aging - induced cooling makes the structure more uniform. The T_3-processed sample has the lowest Icorr 0.314×10^{-6} A/cm², likely due to reversed austenite nucleation and growth increasing Ni content, strengthening the passivation film. Under T4 aging, the sample has the lowest Ecorr and a small corrosion tendency, but the highest Icorr 0.411×10^{-6} A/cm². The growth of N_3Ti and the increase in reversed - austenite volume fraction disrupt the structure, resulting in the worst corrosion resistance.

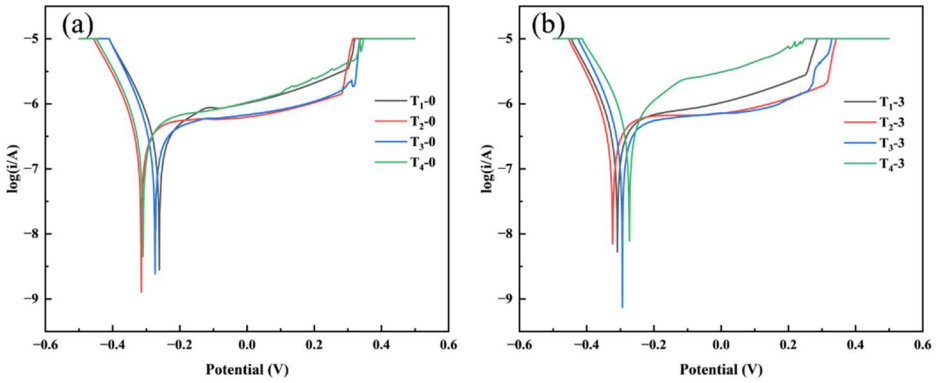

Fig.3 Polarization curves of 1RK91 after conventional aging: (a) Solution treatment, (b) ECAP-3

Fig. 3(b) shows the polarization curves of 1RK91 stainless steel after conventional aging following ECAP-3. Analysis reveals a passivation region under all test conditions. The electrochemical parameters of ECAP-3 samples post-aging are in Table 5. Compared to non-aged samples, aged ones have a lower corrosion current density, with similar corrosion potential. For pitting potential, only the T_4 process has a lower value than non - aged samples; others are higher.

Overall, considering corrosion potential, pitting potential, and self-corrosion current density, the corrosion resistance of ECAP-3 samples after conventional aging is significantly better than non - aged and solution-aged samples. This can be explained in two ways. First, ECAP increases steel's dislocation density, and the deformation-induced martensitic transformation provides more nucleation sites for intermetallic compound precipitation during aging. Second, deformed martensite divides retained austenite and refines the microstructure, making it more homogeneous and enhancing corrosion resistance.

ISSN: 2414-1895 DOI: 10.6919/ICJE.202504_11(4).0021

After aging, the T_3 process has the lowest self - corrosion current density 0.392×10^{-6} A/cm², while T_4 has the highest 0.575×10^{-6} A/cm². This may be because T_4 reaches over-aging temperature, coarsening precipitates and reducing corrosion resistance.

Fig.4 depicts the Nyquist plots of the 1RK91 material subsequent to conventional aging. As can be discerned from the figure, both the solution - treated samples and the ECAP-3 samples display the largest radius of the capacitive reactance arc under the T_3 process. Conversely, under the T_4 process, they present the smallest radius of the capacitive reactance arc. This outcome is in accordance with the measurement findings of the polarization curves.

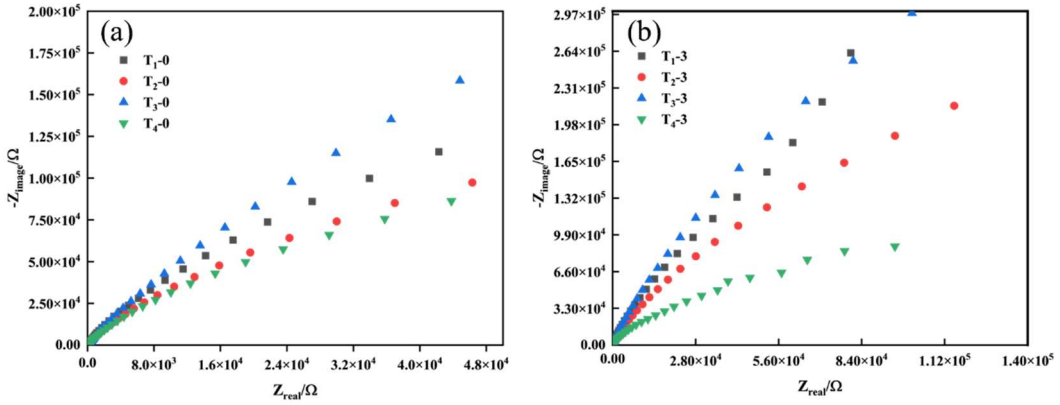

Fig.4 Nyquist Plots :(a) Solution Treatment, (b) ECAP-3

Table 4. Electrochemical params of 1RK91 in conv. aging post- sol. treatment

factor	T_1	T_2	T_3	T_4
$I_{CORR}\times10^{-6}$(A/cm²)	0.323	0.386	0.314	0.411
E_{CORR}(Vvs.SCE)	-0.257	-0.313	-0.271	-0.307
E_b/V	0.271	0.304	0.359	0.356

Table 5. 1RK91 ECAP- 3Conv Aging Electrochem Params

factor	T_1	T_2	T_3	T_4
$I_{CORR}\times10^{-6}$(A/cm²)	0.413	0.471	0.392	0.575
E_{CORR}(Vvs.SCE)	-0.308	-0.325	-0.292	-0.271
E_b/V	0.349	0.356	0.39	0.263

3.3 Effect of Step-Aging Process on the Corrosion Resistance of 1RK91 Stainless Steel

Fig.5(a) presents the polarization curves of 1RK91 stainless steel subsequent to solution and step - aging treatment. The electrochemical parameters for each sample are tabulated in Table 4. The sample treated under the T_8 process exhibits the highest values of corrosion potential (Ecorr) and pitting potential (Eb), accompanied by the lowest self - corrosion current density (Icorr). This set of characteristics indicates that the passive film formed on the surface of the T8 - treated sample has the highest stability.

Conversely, the sample processed under the T_5 process shows relatively lower pitting and corrosion potentials, while its self - corrosion current density is the highest among the samples. This situation

ISSN: 2414-1895 DOI: 10.6919/ICJE.202504_11(4).0021

implies that the passive film on the surface of the T_5-processed sample has the lowest stability, resulting in the poorest corrosion resistance.

When comparing the T_8 and T_4 processes, it is clear that the T_8 process yields the lowest self-corrosion current density, signifying superior corrosion resistance. This can be attributed to the fact that after the solution and step-ging treatment under the T_8 process, the precipitates are fine and evenly distributed. Such a distribution not only inhibits the coarsening of precipitates but also effectively reverses the formation of austenite, thereby significantly enhancing the corrosion resistance of the sample.

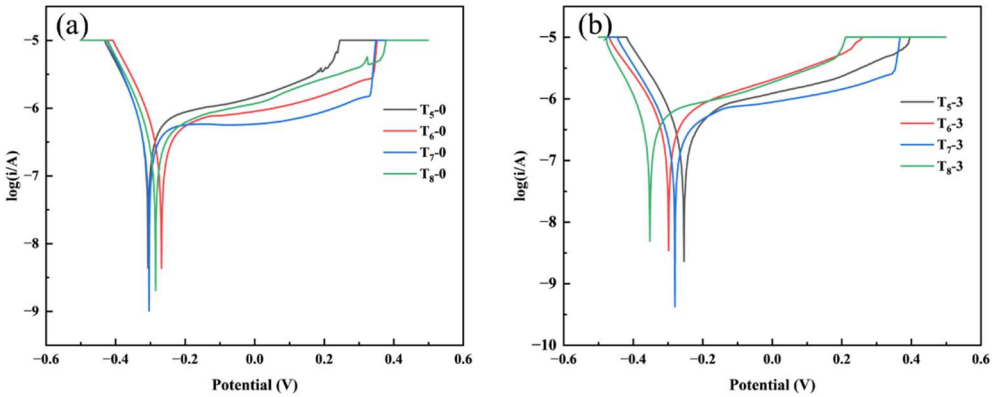

Fig.5 Polarization Curves of 1RK91 after Step-Aging: (a) Solution Treatment, (b) ECAP - 3

Fig.5 shows the polarization curves of 1RK91 stainless steel after step - aging following ECAP-3. For samples treated by T_5 and T_7 processes, the self-corrosion current densities are measured as 0.289×10^{-6} A/cm² and 0.253×10^{-6} A/cm² respectively. Evidently, the T_7-treated sample exhibits the best corrosion resistance. Under the T8 process, the sample's self - corrosion current density reaches 0.439×10^{-6} A/cm² and its pitting potential is 0.261V, indicating the narrowest passivation range and the poorest corrosion resistance. Moreover, the self - corrosion current density after ECAP-3 step-aging is significantly lower than that after conventional aging. This is because step - aging results in fewer precipitated intermetallic compounds (such as Ni_3Ti) in the microstructure. As a consequence, the nickel content in the matrix is relatively high, which stabilizes the passive film and thus enhances corrosion resistance.

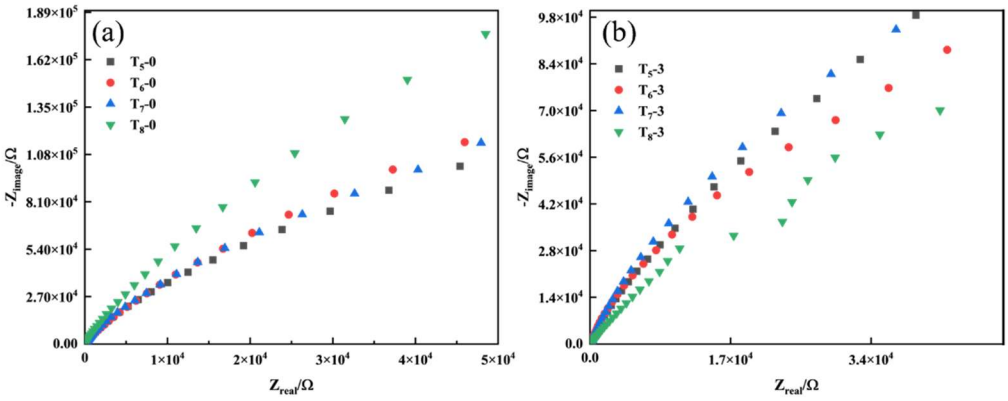

Fig.6 Nyquist Plots of 1RK91 after Step-Aging: (a) Solution - treated, (b) ECAP – 3

Fig. 6(a) shows the Nyquist plots of 1RK91 after step-aging. From the figure, for solution-treated samples, the capacitive reactance arc radius is the largest under the T_8 process and the smallest under

ISSN: 2414-1895 DOI: 10.6919/ICJE.202504_11(4).0021

the T_5 process. This indicates that the material has the best corrosion resistance under T_8 and the worst under T_5. For ECAP-3 samples, the capacitive reactance arc radius is the largest under the T_5 process, showing the best corrosion resistance, while it is the smallest under the T_8 process, indicating the worst corrosion resistance.

Table 6. 1 1RK91 Electrochem Params during Step - aging after Solution Treat

factor	T_5	T_6	T_7	T_8
$I_{CORR}\times10^{-6}(A/cm^2)$	0.527	0.374	0.433	0.362
E_{CORR}(Vvs.SCE)	-0.306	-0.254	-0.304	-0.267
E_b/V	0.291	0.305	0.342	0.371

Table 7. 1RK91 ECAP - 3 Electrochem Param

factor	T_5	T_6	T_7	T_8
$I_{CORR}\times10^{-6}(A/cm^2)$	0.289	0.363	0.253	0.439
E_{CORR}(Vvs.SCE)	-0.251	-0.301	-0.279	-0.357
E_b/V	0.391	0.311	0.315	0.261

4. Conclusion

This chapter explores the impact of different ECAP passes on the corrosion resistance of 1RK91 maraging stainless steel. Conventional and step - aging were applied to solution - treated and ECAP-3 samples, and corrosion - resistance changes were studied. Results are as follows:

For ECAP samples, corrosion resistance rises then falls with ECAP passes. ECAP-1 and ECAP-2 samples have higher corrosion current density and better resistance. ECAP-3 samples, due to large deformation, have high dislocation density, low retained-austenite volume fraction, the largest corrosion current density, and worst resistance.

For conventional aging, solution - treated samples have best corrosion resistance under T_3 and worst under T_4. Similarly, ECAP-3 samples also have best resistance under T_3 and worst under T_4. Moreover, ECAP-3 samples after conventional aging have better resistance than solution-treated ones. Thus, ECAP-3 followed by conventional aging can boost material corrosion resistance.

For step - aging, solution - treated samples have weakest resistance under T_5 and best under T_8 ($T_8 > T_4$). ECAP-3 samples have best resistance under T_5 and worst under T_8. Overall, except for T_8, ECAP-3 samples after step - aging have higher corrosion resistance than solution-treated ones.

References

[1] YADAV S D, EL-TAHAWY M, KALáCSKA S, et al. Characterizing dislocation configurations and their evolution during creep of a new 12% Cr steel [J]. 2017, 134(387-97.

[2] SPRENT J J C I. Circulating T and B lymphocytes of the mouse: I. Migratory properties [J]. 1973,

[3] NIU L, CHENG Y F J A S S. Corrosion behavior of X-70 pipe steel in near-neutral pH solution [J]. 2007, 253(21): 8626-31.

[4] HORITA Z, FURUKAWA M, NEMOTO M, et al. Development of fine grained structures using severe plastic deformation [J]. 2013, 16(11): 1239-45.

[5] TOMOTA Y, OJIMA M, HARJO S, et al. Dislocation densities and intergranular stresses of plastically deformed austenitic steels [J]. 2019,

ISSN: 2414-1895 DOI: 10.6919/ICJE.202504_11(4).0021

[6] SAHARKHIZ H, GHAREHAGHAJI N, NAZARPOOR M, et al. The Effect of Inversion Time on the Relationship Between Iron Oxide Nanoparticles Concentration and Signal Intensity in T1-Weighted MR Images [J]. 2014,

[7] ABRAMOVA M M, ENIKEEV N A, VALIEV R Z, et al. Grain boundary segregation induced strengthening of an ultrafine-grained austenitic stainless steel [J]. 2014, 136(dec.1): 349-52.

[8] HE B B, HU B, YEN H W, et al. High dislocation density–induced large ductility in deformed and partitioned steels [J]. 2017, 357(6355): 1029.

[9] ALVAREZ S M, BAUTISTA A, VELASCO F J C S. Influence of strain-induced martensite in the anodic dissolution of austenitic stainless steels in acid medium [J]. 2013, 69(APR.): 130-8.

[10] IMADE M, ZHANG L, WEN M, et al. Internal Reversible Hydrogen Embrittlement of Austenitic Stainless Steels Based on Type 316 at Low Temperatures; proceedings of the ASME 2009 Pressure Vessels and Piping Conference, F, 2013 [C].

[11] GUTMAN E M, SOLOVIOFF G, ELIEZER D J C S. The mechanochemical behavior of type 316L stainless steel [J]. 1996, 38(7): 1141-5.

[12] LI Z, QIU C, LIU C, et al. The mechanoelectrochemical effect on the electrochemical corrosion of austenitic stainless steel [J]. Journal of Materials Research and Technology, 2023, 24(1203-15.

[13] SINGH R, AGRAHARI S, YADAV S D, et al. Microstructural evolution and mechanical properties of 316 austenitic stainless steel by CGP [J]. Materials Science and Engineering: A, 2021, 812(141105.

[14] SMAGA M, WALTHER F, EIFLER D J A E M. Monotonic and Cyclic Deformation Behaviour of the SiC Particle-Reinforced Aluminium Matrix Composite AMC225xe [J]. 2010, 12(4):

[15] CHENG W, ZENG Y, CUI D, et al. A novel method for the strain strengthening of metastable austenitic stainless steel dome by deep cryogenic forming [J]. 2024, 24(2):

[16] JIANG W, LIU Z, GONG J M, et al. Numerical simulation to study the effect of repair width on residual stresses of a stainless steel clad plate [J]. 2010, 87(8): 457-63.

[17] MASON M B S E, EMAILPROTECTED, EMAILPROTECTED E, et al. Understanding the Mechanism of Secondary Cation Release from the (001) Surface of Li(Ni 1/3 Mn 1/3 Co 1/3)O 2 : Insights from First-Principles [J]. 2023, 127(43): 21022-32.